J. Chem. Sci., Vol. 121, No. 6, November 2009, pp. 1077–1081.

Synthesis of chrysalis-like CuO nanocrystals and their catalytic activity in the thermal decomposition of ammonium perchlorate

JUN WANG[a,b,*], SHANSHAN HE[a], ZHANSHUANG LI[a], XIAOYAN JING[a], MILIN ZHANG[a] and ZHAOHUA JIANG[b]

[a]College of Material Science and Chemical Engineering, Harbin Engineering University, Harbin 150001, P.R. China

[b]College of Chemical Engineering, Harbin Institute of Technology, Harbin 150001, P.R. China

e-mail: junwang@hrbeu.edu.cn

MS received 28 December 2008; revised 4 March 2009; accepted 11 March 2009

Abstract. Chrysalis-like morphologies of CuO have been synthesized in large-quantity via a simple chemical deposition method without the use of any complex instruments and reagents. CuO nanocrystals showed a different morphology at three different temperatures, 25, 60 and 100°C. The particle size, morphology and crystal structure of the samples were characterized by transmission electron microscopy (TEM), scanning electron microscopy (SEM), X-ray diffraction (XRD) and Raman spectra. The catalytic effect of CuO nanoparticles on the decomposition of ammonium perchlorate (AP) was investigated by STA 409 PC thermal analyzer at a heating rate of 10°C min^{-1} from 35 to 500°C. Compared with the thermal decomposition of pure AP, the addition of CuO nanoparticles decreased the decomposition temperature of AP by about 85°C.

Keywords. Nanostructures; ammonium perchlorate; decomposition; catalytic activity.

1. Introduction

Ammonium perchlorate (AP) is one of the main oxidizing agents that have been used in various propellants. The burning behaviour of propellants is highly relevant to the thermal decomposition of AP. The catalysed thermal decomposition of ammonium perchlorate (AP) is remarkably sensitive to metal oxide additives.[1–4] The underlying mechanism of nanoparticle additives in the thermal decomposition of AP still remains unclear, most likely because of the lack of a systematic study about the effects of particle size (or surface area) of CuO nanocrystals on the catalytic activities. For example, Xu *et al*[5] demonstrated that CuO nanocrystals exhibit a particular chemical reactivity due to their high concentration of dislocations and large surface areas. In addition, the different morphologies of nanocrystals are expected to have different effects on the thermal decomposition of AP. Therefore, the synthesis and fabrication of nanostructures with different morphologies and particle size have attracted much attention for research. Well-defined CuO nanostructures with different morphology such as nanoparticles,[6,7] nanoneedles,[8] nanoshuttles,[9] nanoleaves,[10] nanorods,[11,12] nanoribbons,[13,14] nanowires,[15–17] nanoplatelets[18] have been synthesized successfully by a series of methods.

In this paper, CuO nanocrystals were synthesized by the chemical deposition method. With the different reaction temperature, CuO nanocrystals were prepared to show different morphologies. Moreover, with an initial reaction temperature varying from 25°C to 100°C, CuO nanocrystals of different particle size and morphology were synthesized. However, with an initial reaction temperature of 60°C, we found that the resulting products are monodispersed in large quantity and exhibit a chrysalis-like nanocrystalline monoclinic structure. The chrysalis-like CuO nanocrystals were studied as an additive for promoting the thermal decomposition of ammonium perchlorate (AP). With the addition of CuO, the thermal decomposition temperature of AP decreased.

2. Experimental

2.1 *Synthesis of sample*

All the reagents used in this synthesis were of analytical grade and used as received without further

*For correspondence

purification. The typical reaction process for the synthesis of CuO nanocrystals include: 0·02 M $Cu(NO_3)_2$ solution was prepared by dissolving $Cu(NO_3)_2{\cdot}2H_2O$ in 500 ml distilled water. Then, 0·5 g NaOH was added to the solution under constant stirring at three different temperatures, 25, 60 and 100°C. The reaction lasted for 10 min forming a blue or black aqueous solution which was then heated and refluxed with continuous stirring at 100°C for 30 min in a three-necked refluxing pot. During refluxing, the temperature of the solution was controlled by manually inserting an adjustable thermocouple into the refluxing pot. The resultant precipitates were washed with distilled water several times and dried at room temperature.

2.2 *Characterization of sample*

The structure and crystal phases were characterized by power X-ray diffraction (PXRD) with CuKα radiation, wavelength $\lambda = 1{\cdot}54178$ Å (Rigaku D/Max-IIIA). Raman measurement was performed using a Renishaw 1000 model confocal microscopy Raman spectrometer. Morphology and structure of the CuO nanocrystals were characterized using scanning electron microscopy (SEM, JSM-6480A) and transmission electron microscopy (TEM, PHILIPS CM 200 FEG, 160 kV). The thermal behaviour of the CuO nanocrystals was determined using a STA 409 PC thermal analyzer at a heating rate of 10°C min^{-1} from 35 to 500°C in an argon atmosphere and under ambient atmospheric pressure.

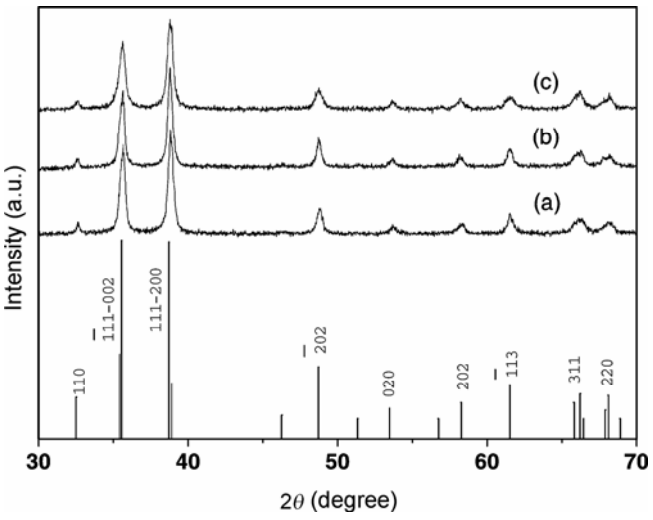

Figure 1. XRD pattern of the CuO nanostructures at different reaction temperature: (a) 25°C; (b) 60°C; (c) 100°C. The (|) vertical lines indicate the position and relative intensity of 48–1548 JCPDS card file diffraction peaks for the monoclinic phase.

2.3 *Catalytic activity measurements*

To evaluate the catalytic activity of the as-prepared CuO nanocrystals, thermogravimetric and different tial scanning calorimetric analysis techniques were applied to investigate the thermal decomposition of a mixture of NH_4ClO_4 and as-prepared CuO nanocrystals from 35 to 500°C under an argon atmosphere, in which the CuO powders and NH_4ClO_4 were thoroughly mixed in mass proportion of 2 : 98. The measurements were performed on a STA 409 PC thermal analyzer at a heating rate of 10°C min^{-1}.

3. Results and discussion

3.1 *Crystal structure and morphology of the as-synthesized CuO*

The structure and chemical composition of all CuO samples synthesized in this work are confirmed with XRD. A typical XRD pattern of all CuO samples is shown in figure 1. The major peaks located at 2θ values of 30–70° correspond to the characteristic diffractions of monoclinic phase CuO (SG: $C2/c$; $a_0 = 4{\cdot}688$ Å, $b_0 = 3{\cdot}423$ Å, $c_0 = 5{\cdot}132$ Å, $\beta = 99{\cdot}50°$; JCPDS 48–1548). No other peak is observed belonging to any impurity, such as $Cu(OH)_2$, Cu_2O, indicating the high purity of the obtained products.

Figure 2 shows the same magnification for SEM image of all CuO samples synthesized in this work. When the initial reaction temperature varied from 25°C to 100°C, CuO nanocrystals with different particle sizes are synthesized. With an initial reaction temperature of 25°C, a large number of CuO flower nanostructures agglomerates formed which are shown in figure 2a. When the initial reaction temperature increased to 60°C, well organized and homogenous chrysalis-like CuO nanostructures formed as shown in figure 2b. With a further increase of temperature, the morphology of CuO nanostructures changes slightly. When the initial reaction temperature reached 100°C, the particle sizes of the CuO nanostructures becomes smaller and their length shorter, as shown in figure 2c.

Figure 3 shows a different magnification for the TEM image of a sample with an initial reaction temperature of 60°C. Figures 3a and b show the repre-

sentative TEM images of the as-prepared CuO aggregates. From figure 3a it can be seen that the product is composed of mostly (~95%) chrysalis-like aggregates. As seen in figure 3b, aggregates are 80–100 nm in breadth and 200–250 nm in length. With careful observation, figure 3c shows that the sample is composed of relatively uniform small particles. A high resolution TEM (HRSEM) image of nanoparticles, as shown in figure 3d, the lattice spacing of 0·25 nm corresponds to a *d* spacing of [110] crystal planes. The corresponding FFT pattern (inset in figure 3d) is consistent with the HRTEM observation.

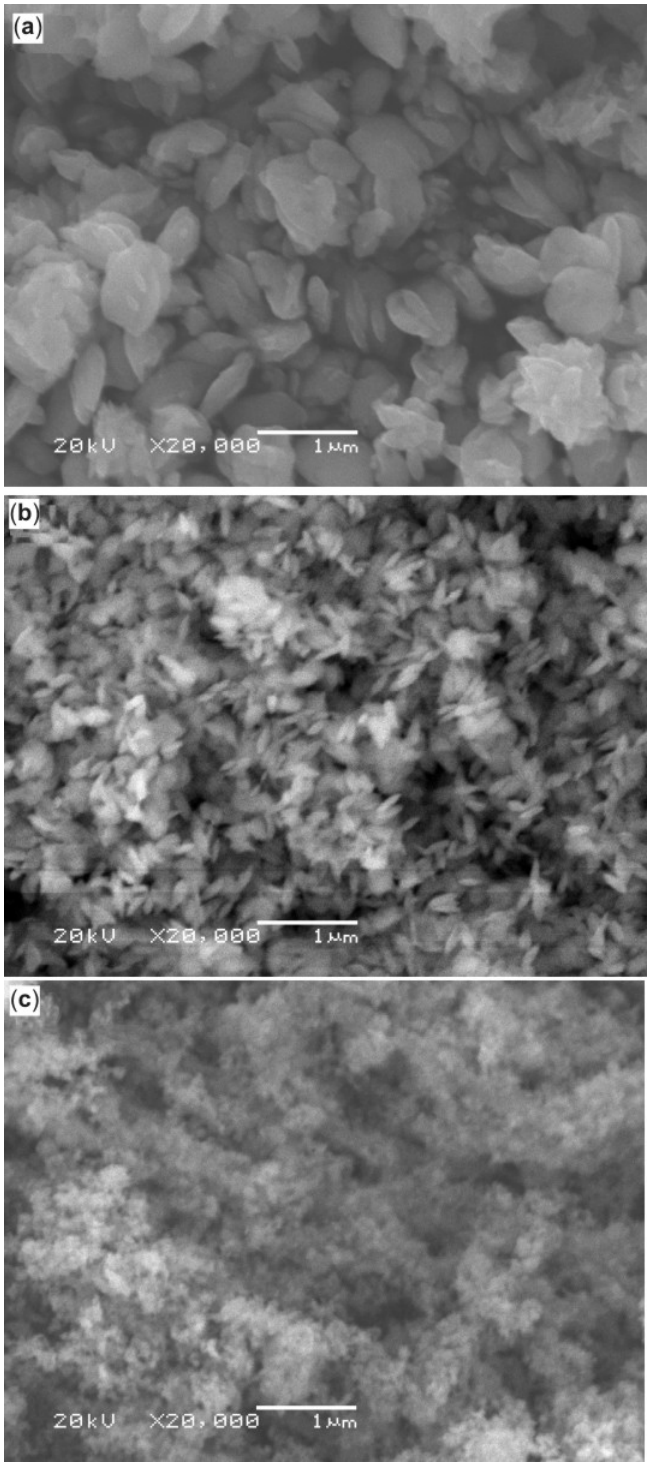

Figure 2. The same magnification SEM image of the CuO nanostructures at different reaction temperature: (**a**) 25°C; (**b**) 60°C and (**c**) 100°C.

Raman spectroscopy, has been widely used as a sensitive probe to investigate the microstructure, namely the local atomic arrangement and vibration, of the nano-sized materials.[19,20] Figure 4 shows the Raman spectra of the as-prepared chrysalis-like CuO nanocrystals. The Raman spectra reveal three main phonon modes in the top of the chrysalis-like CuO nanocrystals, at 276, 327 and 608 cm^{-1}. The Raman peaks are also broadened; the peak at 276 cm^{-1} can be assigned to the Ag mode, while the peaks at 327, 608 cm^{-1} can be assigned to the Bg modes. No Cu_2O modes[21] are present, demonstrating the single phase property of our chrysalis-like CuO nanocrystals.

3.2 *Catalytic properties of the CuO chrysalis-like nanostructures*

To study the catalytic properties of the chrysalis-like CuO nanocrystals, the thermal decomposition of the mixture of as-prepared CuO and NH_4ClO_4 is studied. As shown in figure 5b, the thermal decomposition of pure AP is divided into two exothermic phases: a lower temperature exothermic phase between 310 and 350°C, and a higher temperature exothermic phase between 360°C and 400°C. Figure 5a shows the DSC curve of the mixture of as-prepared CuO and NH_4ClO_4 which displays two peaks at 244·4 and 313·8°C. It is clear that the addition of nano-sized CuO to AP slightly decreases the crystallographic transition temperature of AP, incorporates two small separated exothermic peaks of AP into a strong exothermic peak of AP, and drastically reduces the temperature of the second exothermic peak, indicating a strong catalytic activity on the thermal decomposition of AP.

Further catalytic effect of nano-sized CuO on AP thermal decomposition is carried out by TG. The TG curves for pure AP and AP in the presence of CuO nanoparticles are shown in figure 6. Figure 6a exhibits only one weight loss step and figure 6b exhibits two weight loss steps, which correspond to the exothermic peaks of the DSC curves. The

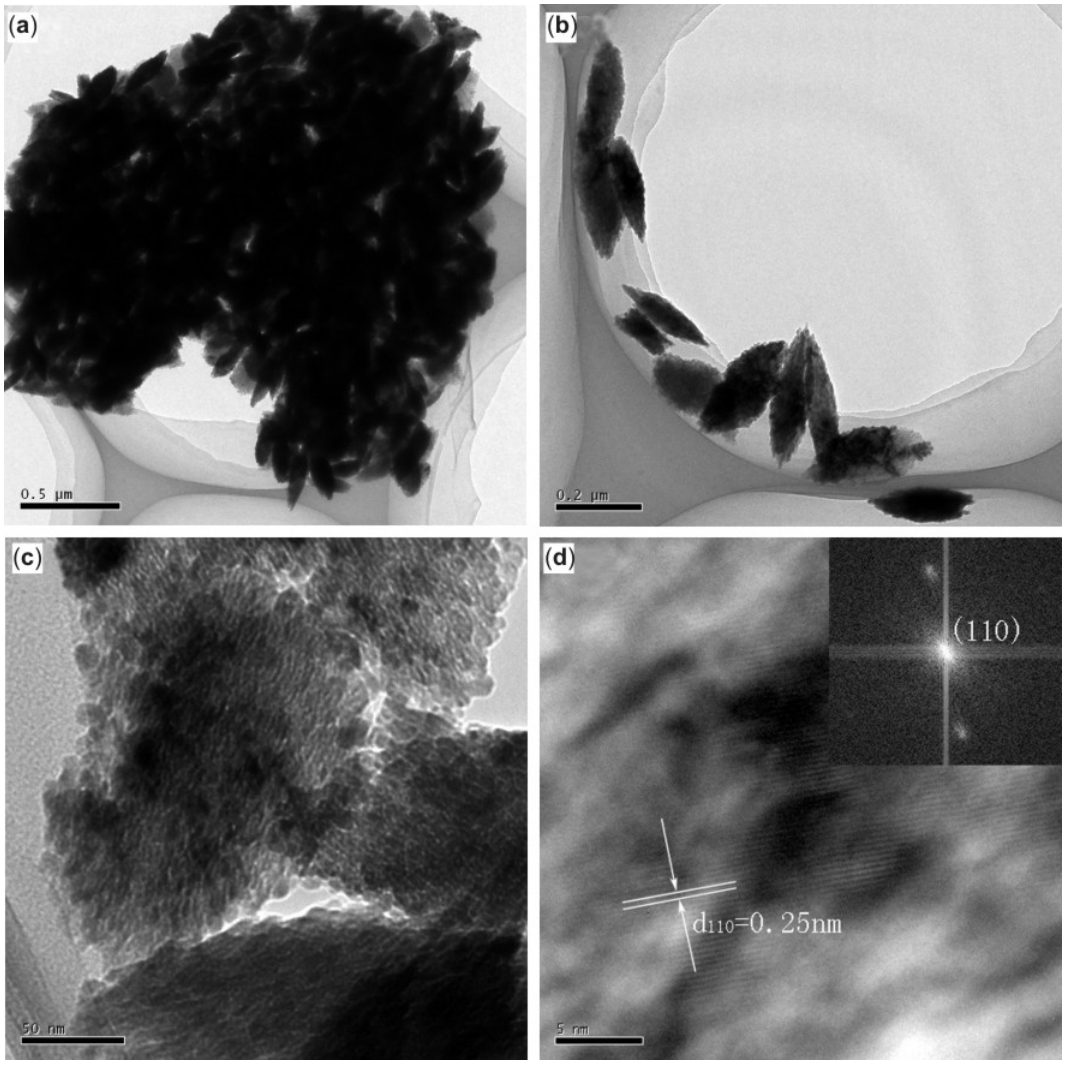

Figure 3. **a–c**, The different magnification TEM image of the sample with an initial reaction temperature of 60°C; (**d**) HRTEM image of the sample showing the difference between two lattice fringes, which is about 0·25 nm. Corresponding FFT pattern (inset) is consistent with the HRTEM observation.

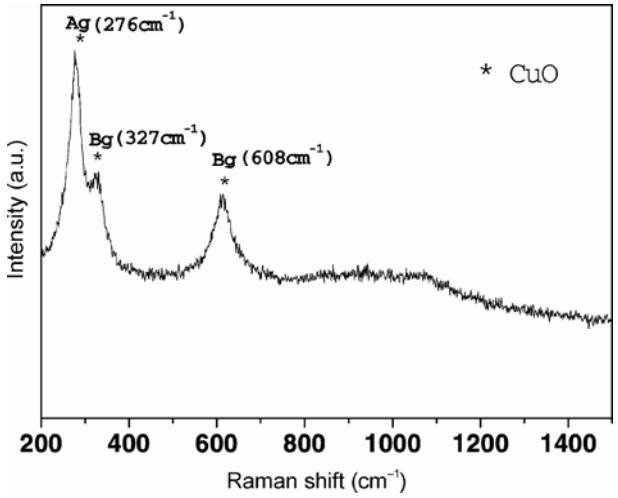

Figure 4. The Raman spectrum of the chrysalis-like CuO nanocrystals.

onsets of thermal decomposition of the two samples are about 300°C, while the end temperatures are about 326 and 411°C, respectively. Adding 2 wt.% CuO nanoparticles allows a decrease of the decomposition temperature of AP by 85°C. These data indicate that addition of CuO nanostructures in AP lead to a significant reduction of the final decomposition temperature of AP.

4. Conclusion

In conclusion, chrysalis-like morphologies of CuO have been synthesized in a large-quantity via a simple solution process without the use of any complex instruments and reagents. CuO nanocrystals showed a different morphology at three different temperatures,

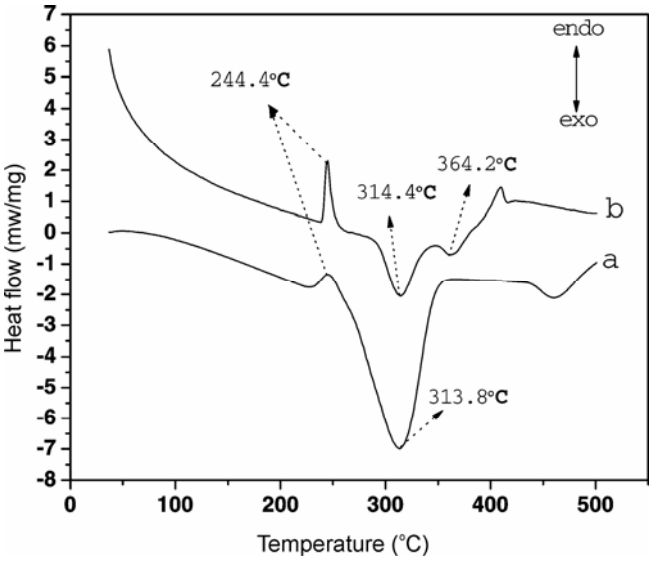

Figure 5. DSC curves for: (a) AP + chrysalis-like CuO nanocrystals; (b) pure AP.

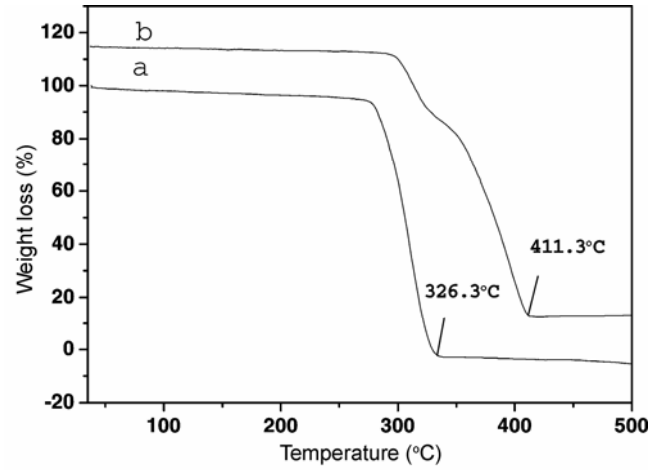

Figure 6. TG curves for: (a) AP + chrysalis-like CuO nanocrystals; (b) pure AP.

25, 60 and 100°C. However, the optimal conditions to prepare chrysalis-like CuO are as follows: At an initial reaction temperature of 60°C, we found that the resulting products are monodispersed in large quantity and exhibit a chrysalis-like nanocrystalline nature of monoclinic structure. Moreover, the addition of nano-sized CuO merges two exothermic peaks of AP (ammonium perchlorate) thermal decomposition into one peak, greatly reducing the high temperature decomposition peak, and drastically increasing the apparent decomposition heat of AP. Hence, there is a great potential for the use of nano-sized CuO in catalytic decomposition of AP.

Acknowledgements

We gratefully acknowledge the support of this research by the Key Technology R&D program of Heilongjiang Province (no.TB06A05), Science Fund for Young Scholar of Harbin City (no. 2004AFQXJ038) and basic research fund for Harbin Engineering University (no. mzj07076).

References

1. Survase D V, Gupta M and Asthana S N 2002 *Progress in crystal growth and characterization of materials*, vol 45, p. 161
2. Yanping Wang, Junwu Zhu, Xujie Yang, Lude Lu and Xin Wang 2005 *Thermochim. Acta* **437** 106
3. Guorong Duan, Xujie Yang, Jian Chen, Guohong Huang, Lude Lu and Xin Wang 2007 *Powder Technol*. **172** 27
4. Lijuan Chen, Liping Li and Guangshe Li 2008 *J. Alloys and Compounds* **464** 532
5. Yanyan Xu, Dairong Chen, Xiuling Jiao and Keyan Xue 2007 *Mater. Res. Bull*. **42** 1723
6. Premkumar T and Geckeler K E 2006 *J. Phys. Chem. Solids* **67** 1451
7. Yueming Li, Jing Liang, Zhanliang Tao and Jun Chen 2008 *Mater. Res. Bull.* **43** 2380
8. Yueli Liu, Lei Liao, Jinchai Li and Chunxu Pan 2007 *J. Phys. Chem.* **C111** 5050
9. Yange Zhang, Shutao Wang, Xuebing Li, Liyong Chen, Yitai Qian and Zude Zhang 2006 *J. Crystal Growth* **291** 196
10. Junwu Zhu, Huiping Bi, Yanping Wang, Xin Wan, Xujie Yang and Lude Lu 2008 *Mater. Chem. Phys.* **109** 34
11. Qi Liu, Yongye Liang, Hongjiang Liu, Jianming Hong and Zheng Xu 2006 *Mater. Chem. Phys.* **98** 519
12. Hongmei Xiao, Luping Zhu, Xianming Liu and Shaoyun Fu 2007 *Solid State Commun.* **141** 431
13. Xinyu Song, Haiyun Yu and Sixiu Sun 2005 *J. Colloid and Inter. Sci*. **289** 588
14. Hongwei Hou, Yi Xie and Qing Li 2005 *Crystal Growth Design* **5** 201
15. Wenzhong Wang, Yan Zhuang and Lin Li 2008 *Mater. Lett*. **62** 1724
16. Yikun Su, Chengmin Shen, Haitao Yang, Hulin Li and Hongjun Gao 2007 *Transactions of Nonferrous Metals Soc. of China* **17** 783
17. Dinesh Pratap Singh, Animesh Kumar Ojha and Onkar Nath Srivastava 2009 *J. Phys. Chem.* **C113** 3409
18. Guifu Zou, Hui Li, Dawei Zhang, Kan Xiong, Chao Dong and Yitai Qian 2006 *J. Phys. Chem.* **B110** 1632
19. Yoshikawa M, Mori Y, Obata H, Maegawa M, Katagiri G, Ishida H and Ishitani A 1995 *Appl. Phys. Lett*. **67** 694
20. Yu T, Zhao X, Shen Z X, Wu Y H and Su W H 2004 *J. Cryst. Growth* **268** 590
21. Reimann K and Syassen K 1989 *Phys. Rev. B Condens Matter* **39** 11113